Peer reviewed version

Link to published version (if available):
10.1016/j.energy.2020.117210

Link to publication record in Explore Bristol Research
PDF-document

University of Bristol - Explore Bristol Research
General rights

Experimental Study with Analysis for a Novel Saturated Activated Alumina Photovoltaic Thermal System

Saber Abdo [1,a,b], Hind Saidani-Scott [2,a], Jorge Benedi[3,c], Mike J. Tierney[4,a]

[1]Saber.abdo@bristol.ac.uk, [2]h.saidani@bristol.ac.uk, [3]jorgebenedi1997@gmail.com, [4]Mike.tierney@bristol.ac.uk

[a] Mechanical Engineering Department, University of Bristol, United Kingdom.

[b] Mechanical Engineering Department, Shoubra Faculty of Engineering, Benha University, Egypt.

[c] School of Engineering Design, Universitat Politècnica de València, Spain.

Abstract

This paper presents a novel photovoltaic thermal system based on water absorption-desorption phenomenon using activated alumina. Experimental work for a promising photovoltaic thermal system that utilise activated alumina tablets as heat absorbing and storing element is presented. Based on the experimental results, electrical, thermal and combined energy efficiencies were calculated and compared with the stand-alone PV panel efficiency. Three identical systems -containing 10 cm depth saturated activated alumina mixed with aluminium mesh cuts- were attached to the back surface of simulated solar panel. The three systems were tested at 600, 800 and 1000 W/m^2 for 6 consecutive working hours, representing sun shining time. Results showed a net energy efficiency of 57% and 53.6% at 600 W/m^2 and 1000 W/m^2 respectively. The electrical efficiency increased by 10.4% and 6.7% at 600 W/m^2 and 1000 W/m^2, respectively, compared with the stand-alone panel. This led to an increase in total energy generation by 309% and 319.5% at 600 W/m^2 and 1000 W/m^2 respectively, compared with stand-alone solar panel.

Key words: PV/T, Solar panels, cooling, materials, activated alumina, saturated

1. Introduction

Affordable, reliable and clean energy is the 7th goal of the United Nation (UN) sustainable development goals as they aim … '*by 2030 to double the improvement in energy efficiency*' (Point 7.3 from [1]). It is also defined as a major goal that is essential to achieve for the other goals. According to the UN website, 13% of the population still don't have access to electricity and 3 billion persons still depend on fossil fuels for their daily usage. Solar energy is an affordable free energy and could be used in many countries that are still relying on fossil fuels for running their electricity generating systems. Incident solar radiation in form of light is used to run solar panels, part of this incident radiation is wasted as heat, raising the temperature of the panel itself [2]. For commercial solar panels, every 1°C rise over the standard test conditions (STC) causes the electrical efficiency to drop by 0.258% [3].

Photovoltaic thermal (PV/T) systems have been studied since 1970 and been developing with new ideas and modern technologies' implementation over the last thirty years [4]. The heat storage has many end-uses like domestic water heating, house heating, food drying and water desalination [5]. These systems are either classified according to the heat transfer mechanism, as active or passive systems or according to the used fluid which is a more specified comparison depending on the heat transfer fluid.

For the active systems, Air PV/T systems that use air streams on the upper and lower surfaces over solar panels were studied and developed (for example, flat plate air collector [6]). In that

example, the aim was to maximise the energy output using unglazed, open loop PV/T system. The system attained an average thermal efficiency of 28-55 % at midday with electrical efficiency range of 10.6% to 12.2%. In a related work on Air PV/T system [7], combined air collector PV/T system with greenhouse air drying system was studied. Electrical, thermal and combined efficiencies of 11.26%, 26.68% and 56.30% were obtained using systems combination. The other common heat transfer agent in forced convection systems is water. Water PV/T systems that utilise water as a cooling/heat storage agent for PV/T systems were well studied. The reported work on this area showed a promising system performance for example, in [8] , five different types of solar panels were tested with surface water flow ; the results showed an overall exergy of 12.15% when using the surface water flow.

Entering the era of Nano technology, with promising nano characteristics substances of high thermal characteristics, Nanofluid-based PV/T were also studied and showed a very good performance compared to water systems. Bellos, E. and Tzivanidis, C. [9], tested concentrated solar panels using parabolic trough using nanofluids as a heat transfer agent and obtained a thermal efficiency of 45% with electrical energy production percentage of 5.8% at 50°C. In a related work, Multi Walls Carbon Nano Tubes were tested for a PV/T system and showed a combined system efficiency of about 61% using 0.075%V. Nano particles concentration [10]. For passive PV/T systems, Phase change materials (PCMs) were the most used substances due to their high latent heat. They were studied as pure substances as well as a mixture with other additives for PV/T systems such as Nano particles additives [11]. The electrical efficiency of 13.7% combined with 72.5% thermal efficiency was achieved. Mousavi, S. et al. [12] studied numerically the effect of combining phase change materials with water PV/T system with a serpentine flow; their system exergy analysis gave an overall exergy efficiency of 16.7%.

Heat pipe PV/T system as a passive PV/T system that utilises the boiling and condensation phenomena of a contained fluid inside the heat pipe was also studied for many end use' applications. A photovoltaic loop heat pipe with a solar assisted heat pump water heating system was investigated and results showed a reduced electricity consumption by 55.7% compared to the conventional water heating system [13]. Fan W. et al., [14] optimised the performance of the life cycle for double pass PV/T solar air heater with heat pipes and showed an annual saving of 925$ - 4606$.

Another technology called Beam splitting technologies were also introduced for concentrated photovoltaic thermal applications and reviewed in [15] based on passive cooling performance for different liquids. The review showed that the standards for beam splitting is not set yet hence the standards for PV/T systems can be used instead for testing such systems.

As a hybrid forced-Natural convection PV/T system, Nanofluids were tested with PCM thermal battery for residential applications and the system was able to cover 77% of the electrical residential load and 27% of the thermal load [16].

Water absorption mediums- like heat spreaders in conjunction with cotton wick structure -were recently studied for cooling solar panels [17]; however, waste/unusable heat and experiments repeatability were major issues in this work. Recently in 2019, Kandilli C. et al [18] proposed an experimental study for thermal system integrated with natural zeolite for heat management based on different passive methods including utilising paraffin, stearic acid and zeolite. The overall energy efficiency of their proposed system recorded a value of 33%, 37%, and 40% when using paraffin, stearic acid and zeolite in PV/T system.

From the literature presented, it is clear that passive PV/T systems are more sustainable to be considered rather than forced systems due to less energy consumption for medium forcing e.g. for the pump or the fan. Research field on using the water absorption-desorption technique for PV/T system is not developed yet . This paper is one of the first to address a potential research on such systems performance, energy analysis and overall efficiency improvement.

2. Research theory

The novelty of the proposed system is to allow water desorption in form of water vapour to the surrounding by natural convection. In the same time, the temperature of activated alumina increases by recovering and storing part of the removed heat, as shown in figure 1. Activated alumina was chosen because its ability to withstand high temperature and its water absorptivity. The water goes into the bores of the inner particles and contained inside with no leakage opportunity in normal conditions but allows the water vapour to escape if applied the adequate heat amount on the system. It can also adsorb water up to 30% of its weight in normal atmospheric temperature and allows to evaporate significant portion of it when temperature increases [19].
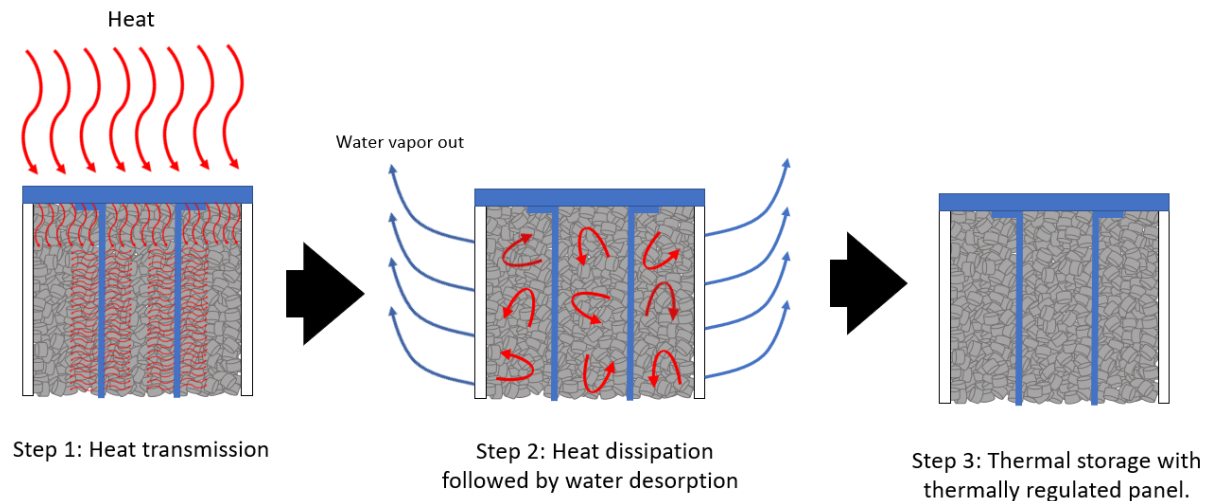

Figure 1: A schematic diagram of the proposed thermal regulation/heat storage process

From this diagram, it can be noted that two outputs can be obtained from this system. The first one, is the thermal regulation for solar panels and the second is the thermal heat storage inside the activated alumina particles themselves that can be used for other thermal applications. Activated alumina is a promising substance for this type of systems due to its thermal characteristics and its suitability for the periodic cycle proposed in figure 2 below.
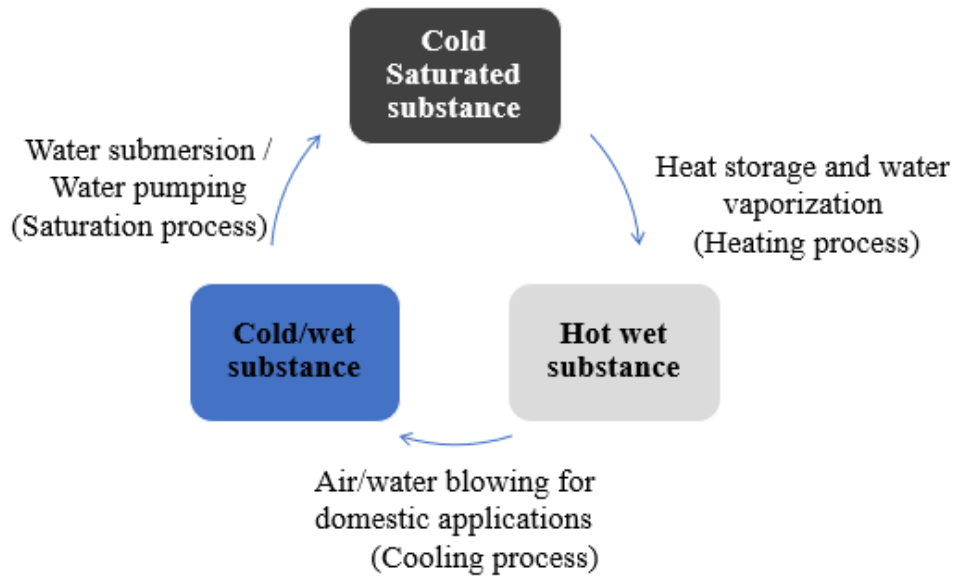
Figure 2: Proposed cycle for activated alumina PV/T system.

3. Experimental setup

In order to test the system performance, Ten-centimetre depth activated alumina, with 1%wt. metal mesh cuts with two fins insertion was used as an attached block below the simulated panel. Experiments were run several times with the same test rig for energy (electrical and thermal) analysis which is the main objective of this research. Activated alumina tablets with 7 mm diameter and 5 mm depth were used due to their porosity and thermal characteristics.

Solar panels were simulated using three blue coated Aluminium plates of emissivity 90% of similar characteristics of PV panels based on experimental results [20], [21] which have been widely used in similar researches [22] and [23]. Table 1 shows the characteristics of activated alumina and the simulated solar panel.

Table 1: Material specifications

Item	Specifications	
Activated Alumina	Supplier	Laporte Industrial Limited
	Shape – dimensions	Tablets – 7mm dia., 5 mm depth.
	Static water absorption	30 +/- 1 %wt.
	Total pore volume	0.5 cc/g
	Dry density	700 kg/m^3
	Specific heat capacity	1 kJ/kg.K
Simulated Solar panel specifications	Model	Trina, ALLMAX- PD05.08
	Type	Multi crystalline solar panels
	Temperature coefficient	0.41 %/^{o}C
	Module reference efficiency	17.1%
	Emissivity	0.9

Indoor test rig was fabricated using 6x1000 W halogen lamps with 2x3 kW variable transformers for changing light intensity. Three radiations of 600, 800 and 1000 W/m^2 were selected, representing minimum, mean, and maximum radiation intensities reaching earth from sun [10].

As seen in diagram shown in figure 3, only the transmitted part of the radiation was given to the plate by subtracting the percentage electricity generation. This radiation intensity represents the accumulative heat to be removed and stored through the activated alumina attachment below the panel. This transmitted portion was calculated based on equation 1 and 2.

$$Q_{trans.} = I_{total} - E_{generated} \qquad \text{Equation 1}$$

$$E_{gnereated} = I''_{total} * A_s * \eta_{electric} \qquad \text{Equation 2}$$

Where:

$Q_{trans.}$: Transmitted heat to be removed = actual input to the system W

I_{total} : Total radiation input to PV panels W

$E_{generated}$: estimated electrical energy output from PV panels   W

I''_{total}:total radiation flux into the PV panel W/m^2

A_s: Solar panel area m^2

$\eta_{electric}$; Estimated electrical efficiency based on operating temperature from Evans equation (equation 3) [23]

$$\eta_{elec.} = \eta_{T_{ref}}\left[1 - \beta_{ref}\left(T_{Panel} - T_{ref}\right)\right] \qquad \text{Equation 3}$$

Where, $\eta_{T_{ref}}$ is the efficiency of solar panel at (STC) and it was assumed 17.1% based on Trina solar multi-crystalline PV panel data sheets (ALLMAX- PD05.08). Temperature coefficient β_{ref} is also taken as 0.0041 C^{-1} for silicon PV panels based on [23], T_{ref} is the standard test temperature (25 °C).
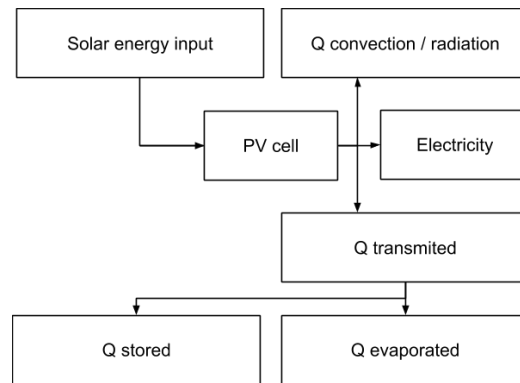

Figure 3: Heat balance of the proposed system

Figure 4 represents a schematic diagram for the complete test rig planned for this experiment.
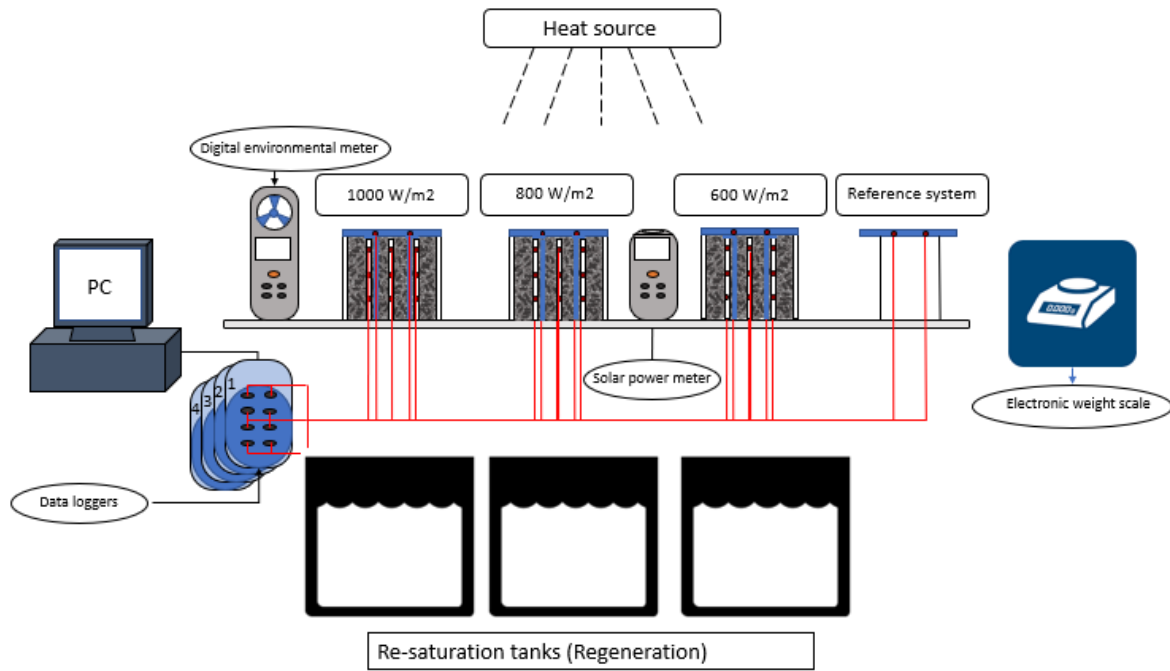
Figure 4: Schematic drawing for the complete test rig.

Three perforated acrylic boxes of dimensions (15x15) cm and 10 cm depth filled with activated alumina-aluminium mesh cuts were manufactured in order to test the performance of the proposed system under different radiation. Experiments were repeated in order to minimise errors for system analysis and to ensure the reusability of the activated alumina as a heat storage and cooling agent. In each system, 11 K-type thermocouples were attached in the array shown in the schematic diagram for measuring the temperature at different depths from the top layer and to measure the cooling effect on the simulated solar panel. Figure 5 represent box filling with activated alumina before applying the simulated panel and thin aluminium layers were used to fill the existing gap between the activated alumina tablets and the plate.

Figure 5: Filled box with activated alumina before fins insertion and plate fixation.

Figure 6 shows the full test rig used in experiments that is held in the Thermofluid Lab at the University of Bristol, UK.
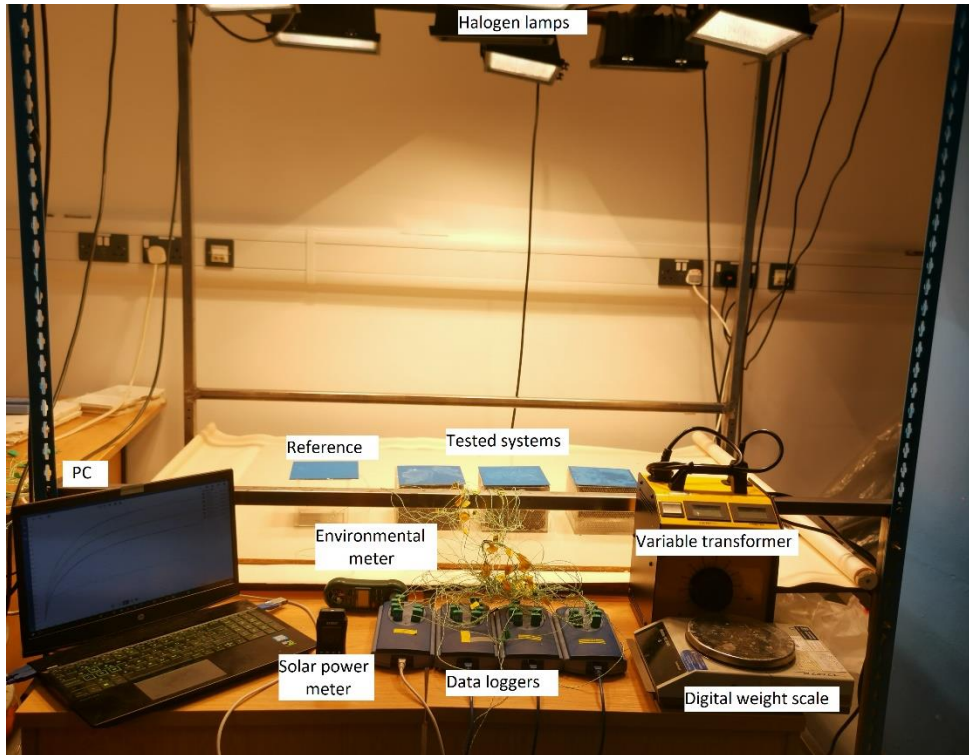
Figure 6: Complete test rig.

The temperature within the test area was controlled by the lab ventilation system and was set between (31 to 35)°C. The relative humidity was recorded to be between 40-60 %.

Solar radiation was calibrated in the test area using calibrated solar power meter and the radiation was controlled using two variable transformers. Air velocity (Set to zero), relative humidity and ambient temperature were measured at the same test location using a digital environmental meter. Instruments specifications used in these experiments are given in table 2.

Table 2: Specification of measuring devices

Thermocouples	Type	K-Type
	Range	0 to 275 °C
Weight scale	Range	0 to 4 kg
	Accuracy	±10 g
Thermographic camera	Type	Flir E6
	Range	-20 to 250 °C
	Accuracy	±2 %
Data Acquisition system	Type	Pico Technology TC-08
	Accuracy	±0.2 %
	Range	-270 to 1370 °C
Solar power meter	Type	Extech SP505
	Range	0 to 3999 W/m^2
	Accuracy	±10 W/m^2

Activated alumina was submerged in water for 3 hours before starting the experiments. Afterwards, each experiment was run daily for 6 continuous hours, simulating sun hours-time.

The experiments were repeated, data were collected and inserted in Microsoft Excel file for analysing data and calculating the heat storage and calculating electrical efficiency from Evans equation. Results were scaled to 1 m^2 solar panel for calculating the daily heat storage /electrical generation and compared with the un-cooled PV panel output.

Knowing the temperature variation for internal layers of activated alumina at three different depths, the mean temperature and the thermal heat storage were calculated using:

$$E_{stored} = m_{mix} * C_{p_{mix}} * (T_{mean@T+t} - T_{mean@T}) * t \qquad \text{Equation 4}$$

Where:

$T_{mean@T}$ is the mean temperature at the previous time-step.

$T_{mean@T+t}$ is the mean temperature at the current time step.

T is the time step in seconds (15 minutes * 60 S)

$C_{p_{mix}}$: the mixture specific heat and was calculated using:

$$C_{p_{mix}} = \frac{m_D C_{p_D} + m_W C_{p_W} + m_{Al} C_{p_{AL}}}{m_{mix}} \qquad \text{Equation 5}$$

Where subscripts are as follow

D: Dry Activated alumina

W: Water content

AL: Aluminium content.

Thermal efficiency was calculated using the following equation [10]:

$$\eta_{th} = \frac{E_{stored}}{E_{total}} * 100 \qquad \text{Equation 6}$$

Where:

η_{th}: System thermal efficiency.   %

E_{stored}: Stored energy   J

E_{total}: Total energy input to the system   J

Combined system efficiency was also calculated using equation 7 [10].

$$\eta_{combined} = \eta_{th} + \eta_{elec.} \qquad \text{Equation 7}$$

Where:

$\eta_{combined}$: System combined efficiency.   %

$\eta_{combined}$: Calculated electrical efficiency   %

And panel temperature reduction by:

$$\Delta T_{avg} = \frac{\sum_1^n (T_{uncooled} - T_{cooled})}{N} \qquad \text{Equation 8}$$

Where:

N: Number of measurements

Efficiency increment was calculated at each measurement using the following formula:

$$\Delta\%_{increase} = \frac{\eta_{combined} - \eta_{elec.ref}}{\eta_{elec.ref}} \% \qquad \text{Equation 9}$$

With:

$\eta_{elec.ref}$: The reference system electrical efficiency

The average increment over the test period was calculated using:

$$\Delta\%_{avg} = \frac{\sum_1^n \Delta\%_{increase}}{N} \qquad \text{Equation 10}$$

4. Experimental errors and uncertainties

Calibrated instruments were used in the experiment and the percentage uncertainty was calculated using [24] as follow:

$$e_r = \left[\left(\frac{\partial R}{\partial V_1} e_1 \right)^2 + \left(\frac{\partial R}{\partial V_2} e_2 \right)^2 + \cdots + \left(\frac{\partial R}{\partial V_n} e_n \right)^2 \right]^{0.5} \qquad \text{Equation 11}$$

While:

$V_1, V_2, and\ V_n$ are the variables affecting the results obtained from experiments.

$e_1, e_2, and\ e_n$ are errors associated with the corresponding variable numbers.

From table 2, the uncertainty was calculated as follow

$e_R = [(0.036)^2 + (0.25)^2 + (0.7)^2 + (0.012)^2 + (0.025)^2]^{0.5} = \pm 0.898$

The uncertainty was less than the permittable value for low hazard application which is 5%.

5. Results and Discussion

Systems were tested under 600, 800 and 1000 W/m^2 radiation intensities and the temperature of the cooled simulated panel were recorded as well as the temperature at equidistance thermocouples positions as illustrated above and compared to the reference system running under the same meteorological conditions. The recorded temperature at the cooled plate, 2.5 cm (Top raw), 5 cm (Middle raw) and 7.5 cm (Bottom raw) from the plate at the three different radiations were plotted against the uncooled system in figure 7, 8 and 9 at 600, 800 and 1000 W/m^2 radiation respectively.
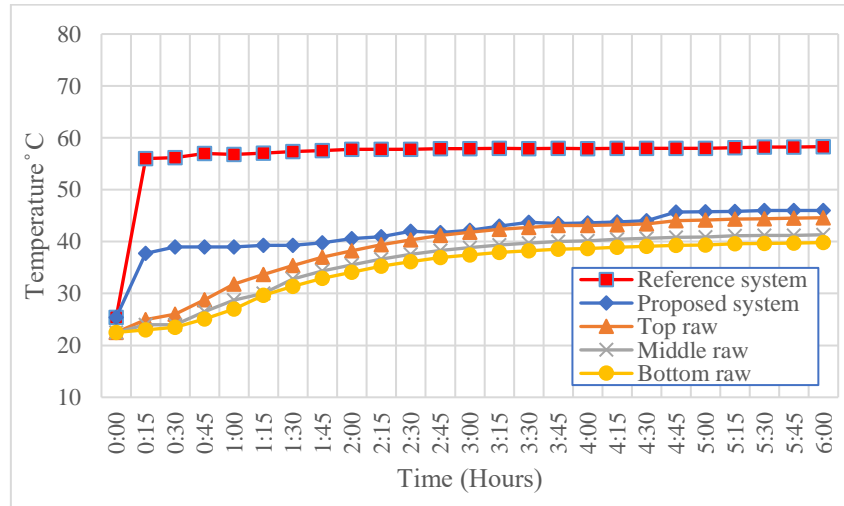

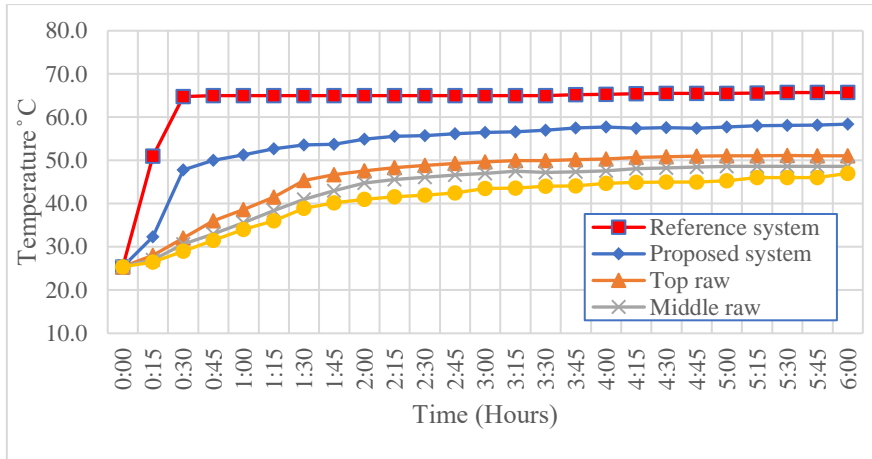Figure 7: Temperature distribution at different levels at 600 W/m^2.

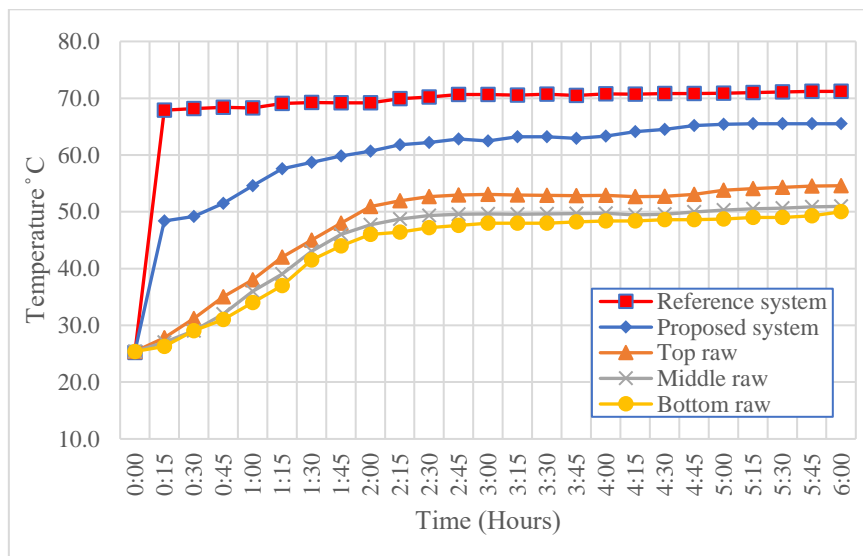Figure 8: Temperature distribution at different levels at 800 W/m^2.

Figure 9: Temperature distribution at different levels at 1000 W/m^2.

From figure 7 to 9 above, it can be noted that the system had its higher performance as a cooling system at 600 W/m^2 because the system was able to store the heat within the activated alumina itself and didn't reach higher temperatures that allows the water vapour to escape. Also, the temperature of the top layer approached the plate temperature because of the low radiation and less natural air/water vapour circulation inside the boxes.

With increasing radiation, the gap between the plate temperature and other layers temperature increases; this is due to the heat transmission throughout the activated alumina layers and the plate. Moreover, the water desorption and the natural air circulation increased due to the higher temperature difference between the plate and the bottom layer that reached 18˚C and 21˚C at 800 and 1000 W/m^2 respectively.

Figures 10, 11 and 12 represent the output efficiencies -including thermal, electrical and combined efficiencies- for the proposed system compared to the electrical efficiency of uncooled solar panels running under the same meteorological conditions.
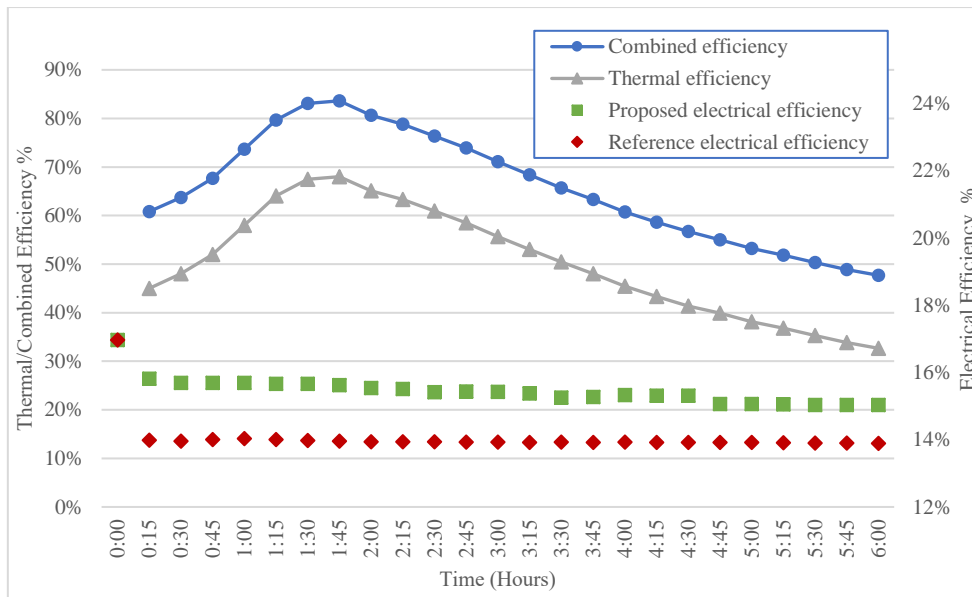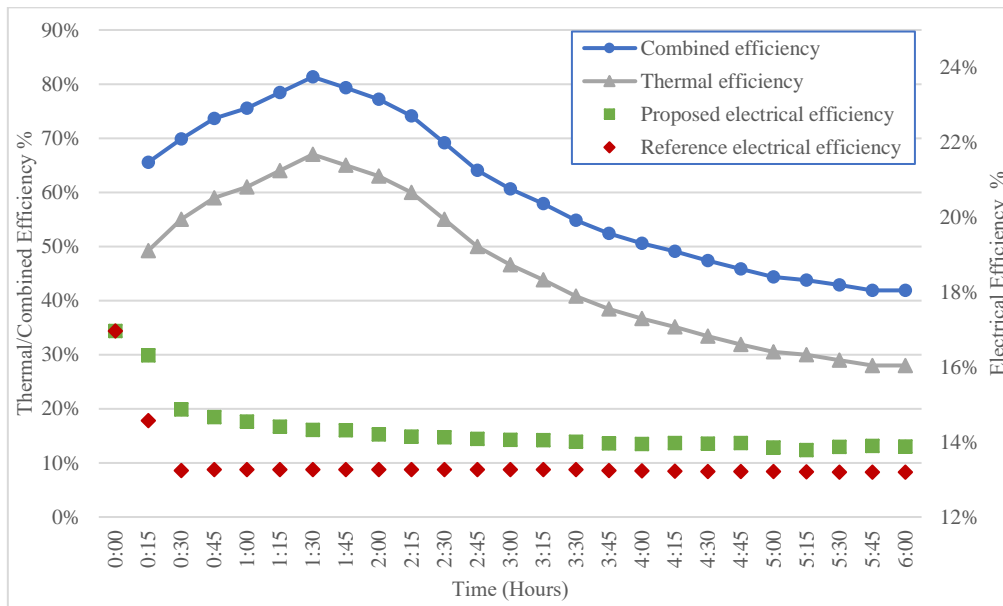
Figure 10: System efficiencies at 600 W/m^2.

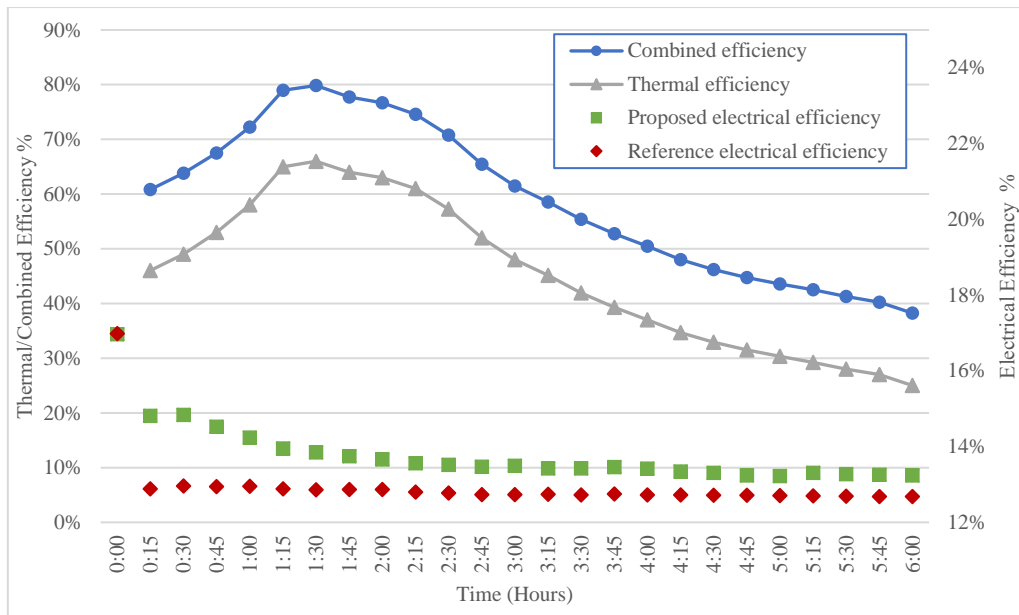Figure 11: System efficiencies at 800 W/m^2.

Figure 12: System efficiencies at 1000 W/m^2.

It can be noted that the proposed system gives better performance and energy utilisation at all tested radiations compared to the reference system. Also, the maximum efficiency obtained using the proposed system occurs at earlier times using higher solar radiations which is expected to happen due to the higher heat transmission and heat storage. After the peak time, the trend for the combined efficiency decreases sharply in the case of higher radiations due to water vapour escaping with the loss of heat.

Figures 13, 14 and 15 show the energy production per day per unit area at different radiation using the proposed system compared to total energy input and stand-alone solar panels production.
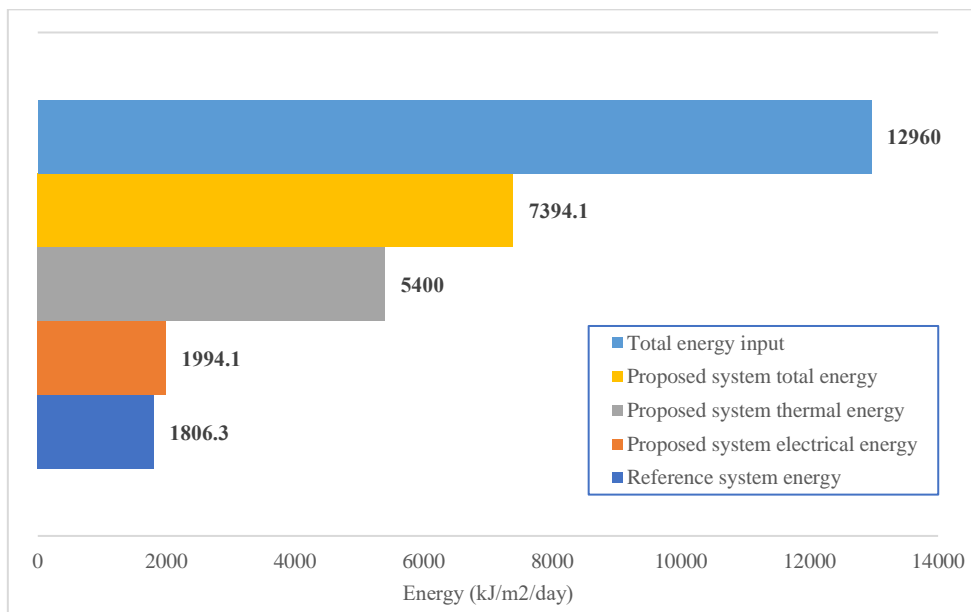

Figure 13: Energy input/generated per m^2 per day at 600 W/m^2 radiation.
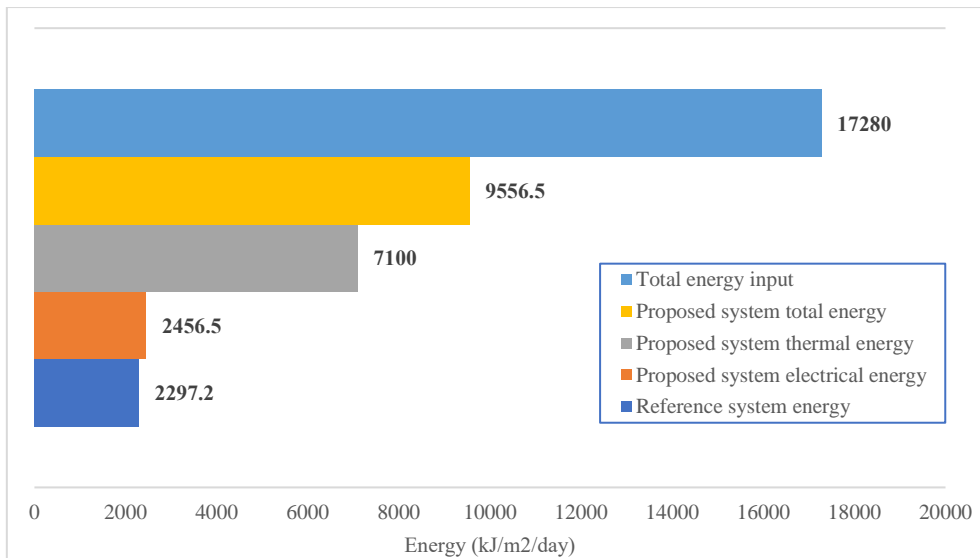
Figure 14: Energy input/generated per m^2 per day at 800 W/m^2 radiation.
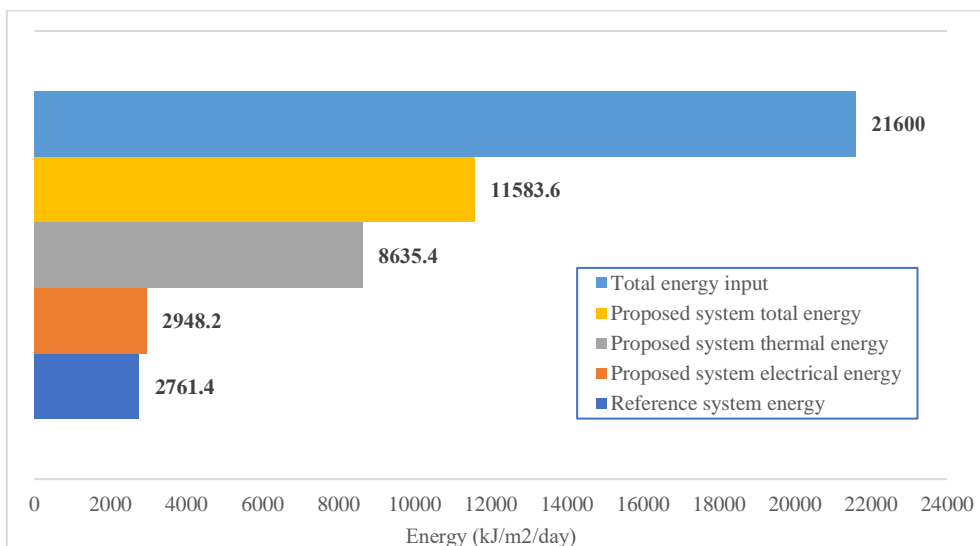

Figure 15: Energy input/generated per m^2 per day at 1000 W/m^2 radiation.

From the above figures, it can be seen clearly that the proposed system gives a promising energy efficiency including electrical and thermal energies that are supposed to be lost without the usage of the activated alumina PV/T system. Table 3 shows the proposed system efficiencies at different radiations compared with the stand-alone PV panels. The system feasibility for application in terms of energy efficiency is promising, compared to using standalone solar panels. This system will be able to give more energy utilisation as it increased the total energy generation by 309% and 319% at 600 W/m^2 and 1000 W/m^2 solar radiations respectively. This energy increase is composed of increased electrical energy generation and thermal energy stored for possible domestic applications. Figure 16 shows a diagram concluding different efficiencies obtained from the system at different radiation intensities.
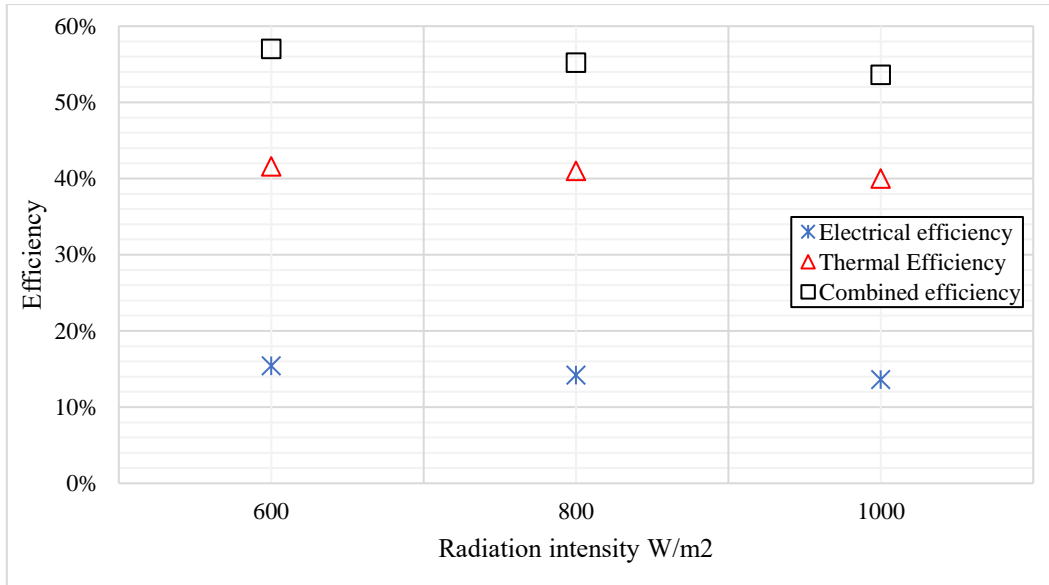
Figure 15: System efficiencies variation at different radiation intensities.

Table 3: Summary of system proposed system performance compared with stand-alone solar panels

Solar radiation	Comparison Factor	Value
600 W/m²	Panel temperature reduction (Avg.)	14.9˚C
	Reference electrical efficiency (Avg.)	14%
	Proposed electrical efficiency (Avg.)	15.4%
	Proposed thermal efficiency (avg.)	41.6%
	Proposed combined efficiency (Avg.)	57%
	Percentage increase of electric energy generation	10.4 %
	Total increase in energy generation	309 %
800 W/m²	Panel temperature reduction (Avg.)	9.5˚C
	Reference electrical efficiency (Avg.)	13.2%
	Proposed electrical efficiency (Avg.)	14.2%
	Proposed thermal efficiency (avg.)	41%
	Proposed combined efficiency (Avg.)	55.3%
	Percentage increase of electric energy generation	7%
	Total increase in energy generation	316%
1000 W/m²	Panel temperature reduction (Avg.)	8.9˚C
	Reference electrical efficiency (Avg.)	12.8%
	Proposed electrical efficiency (Avg.)	13.6%
	Proposed thermal efficiency (avg.)	40%
	Proposed combined efficiency (Avg.)	53.6%
	Percentage increase of electric energy generation	6.7%
	Total increase in energy generation	319.5%

For restoring the thermal energy overnight, three methods can be used. The first method is the re-saturation tank filled with water which will give two benefits: the first one is re-saturating the activated alumina and the second benefit is acquiring heat within the water inside the tank. The second method is water flow over the hot activated alumina which will give the same benefits as the first method but will require either external pump to force the fluid or hanged water tank over the system with flow control valves. The last method consists of blowing air with a fan over the activated alumina for air heating applications. Figure 16 shows different proposed methods for heat utilisation.
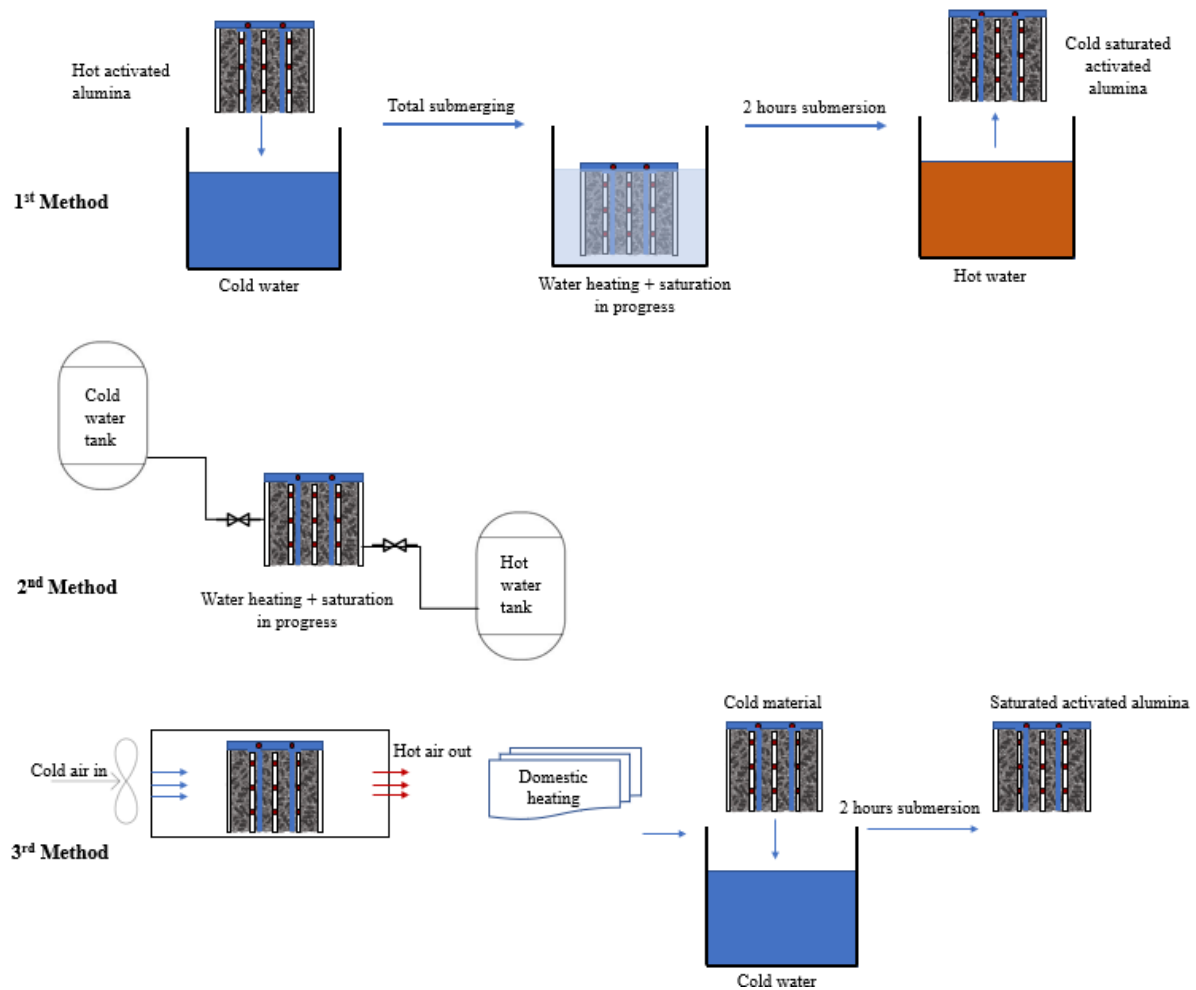

Figure 16: Proposed heat extraction / activated alumina re-saturation methods

Table 4 represents a comparison between the proposed system and the reported systems in the literature. From this comparison, it is clearly that the proposed system has a lot of advantages over the other systems including, availability in commercial and natural scale, suitability for different climates, low maintenance and no power consumption. Furthermore, the system can be used for multiple end use application with relatively medium cost compared to other types of PV/T systems.

Table 4: Comparison between the proposed systems and other systems.

According to	Proposed PV/T	Air PV/T [7]	Water PV/T [8]	PCM PV/T [12]	Nanofluid PV/T [10]	Heat pipe PV/T [14]	Beam split PV/T [15]
Medium availability	Natural / Commercial	Natural	Naturally	Commercial	Commercial	Commercial	Commercial

Thermal characteristics	Medium	Low	Medium	Low	High	Fluid dependent	Fluid dependent
Maintenance	low	low	high	low	high	high	low
Climate conditions suitability	Suitable for all climates	Suitable for cold climates	Suitable for all climates	Suitable for all climates	Suitable for all climates	Suitable for all climates	Suitable for clear skies
Leakage risk	No risk	No risk	High risk	High risk	High risk	High risk	High risk
Thermal expansion risk	No risk	No risk	Medium risk	High risk	Medium risk	High risk	Medium risk
Agglomeration risk	No risk	No risk	No risk	No risk	High risk	No risk	No risk
Corrosion risk	yes	No	yes	No	yes	yes	yes
Technology development	Developed	Developed	Developed	In development	In development	In development	In development
End uses	Multiple	Limited	Limited	Multiple	Multiple	Multiple	Limited
Heat extraction	Indirect	Direct	Direct	Indirect	Indirect	Indirect	Indirect
Heat storability	Yes	No	Yes	Yes	Yes	Yes	Yes
Power consumption	Not required	Required for active type	Required for active type	Not required	Required for active type	Not required	Not required
Weight	Heavy	Light	Heavy	Heavy	Heavy	Heavy	Heavy
Suitability for tracking	Suitable	Suitable	Not suitable	Suitable	Not suitable	Suitable	Suitable
Initial cost	Low	Low	High	High	High	High	Low

6. Conclusion

Saturated activated alumina, which is commercially known as activated alumina, was mixed with Aluminium cuts and tested as a double role agent (heat removal agent for cooling solar panels and heat storage medium for the absorbed heat). Three solar radiations were simulated at ambient temperature range between $31 - 35\,^\circ$C. The system showed a very good capability of removing undesired heat from the back surface of the simulated solar panel reducing its temperature by 14.9 and $8.9\,^\circ$C at 600 and 1000 W/m^2 respectively. From another perspective, the system was able to store (40 - 41.6) % of incident radiation as a form of heat within the activated alumina itself raising the energy efficiency from 14% to 57% for the same setup area at 600 W/m^2 and from 12.8% to 53.6 % at 1000 W/m^2 radiation.

Acknowledgement

References

[1] https://www.un.org/sustainabledevelopment/energy/ last visited 20th June 2019.

[2] Physics Today 60, 3, 37 (2007); doi: 10.1063/1.2718755.

[3] Amelia, A.R., Y.M. Irwan, W.Z. Leow, M Irwanto, I. Safwati and M. Zhafarina. (2016), "Investigation of the Effect Temperature on Photovoltaic (PV) Panel Output Performance". International Journal on Advanced Science Engineering Information Technology, Vol.6, No.5, 2016, Page 684.

[4] Joshi, S. S. and Dhoble, A. S. (2018) "Photovoltaic -Thermal Systems (PV/T): Technology Review and Future Trends," Renewable and Sustainable Energy Reviews, 92, pp. 848–882. doi: 10.1016/j.rser.2018.04.067.

[5] Sultan, S. M. and Ervina Efzan, M. N. (2018) "Review on Recent Photovoltaic/thermal (PV/T) Technology Advances and Applications," Solar Energy, 173, pp. 939–954. doi: 10.1016/j.solener.2018.08.032.

[6] Bambrook, S. M. and Sproul, A. B. (2012) "Maximising the Energy Output of a PVT Air System," Solar Energy, 86(6), pp. 1857–1871. doi: 10.1016/j.solener.2012.02.038.

[7] Tiwari, S., Agrawal, S. and Tiwari, G. N. (2018) "PVT Air Collector Integrated Greenhouse Dryers," Renewable and Sustainable Energy Reviews, 90, pp. 142–159. doi: 10.1016/j.rser.2018.03.043.

[8] Tomar, V., Tiwari, G. N., Bhatti, T. S. and Norton, B. (2018) "Thermal Modeling and Experimental Evaluation of Five Different Photovoltaic Modules Integrated on Prototype Test Cells with and Without Water Flow," Energy Conversion and Management, 165, pp. 219–235. doi: 10.1016/j.enconman.2018.03.039.

[9] Bellos, E. and Tzivanidis, C. (2019) "Investigation of a Nanofluid-Based Concentrating Thermal Photovoltaic with a Parabolic Reflector," Energy Conversion and Management, 180, pp. 171–182. doi: 10.1016/j.enconman.2018.11.008.

[10] Abdallah, S. R., Saidani-Scott, H. and Abdellatif, O. E. (2019) "Performance Analysis for Hybrid PV/T System Using Low Concentration MWCNT (water-Based) Nanofluid," Solar Energy, 181, pp. 108–115. doi: 10.1016/j.solener.2019.01.088.

[11] Al-Waeli, A. H. A., Sopian, K., Chaichan, M. T., Kazem, H. A., Ibrahim, A., Mat, S. and Ruslan, M. H. (2017) "Evaluation of the Nanofluid and Nano-Pcm Based Photovoltaic Thermal (PVT) System: An Experimental Study," Energy Conversion and Management, 151, pp. 693–708. doi: 10.1016/j.enconman.2017.09.032.

[12] Mousavi, S., Kasaeian, A., Shafii, M. B. and Jahangir, M. H. (2018) "Numerical Investigation of the Effects of a Copper Foam Filled with Phase Change Materials in a Water-Cooled Photovoltaic/thermal System," Energy Conversion and Management, 163, pp. 187–195. doi: 10.1016/j.enconman.2018.02.039.

[13] Li, H. and Sun, Y. (2019) "Performance Optimization and Benefit Analyses of a Photovoltaic Loop Heat Pipe/solar Assisted Heat Pump Water Heating System," Renewable Energy, 134, pp. 1240–1247. doi: 10.1016/j.renene.2018.09.055.

[14] Fan, W., Kokogiannakis, G. and Ma, Z. (2019) "Optimisation of Life Cycle Performance of a Double-Pass Photovoltaic Thermal-Solar Air Heater with Heat Pipes," Renewable Energy, 138, pp. 90–105. doi: 10.1016/j.renene.2019.01.078.

[15] Ju, X., Xu, C., Han, X., Du, X., Wei, G. and Yang, Y. (2017) "A Review of the Concentrated Photovoltaic/thermal (cpvt) Hybrid Solar Systems Based on the Spectral Beam Splitting Technology," Applied Energy, 187, pp. 534–563.
doi: 10.1016/j.apenergy.2016.11.087.

[16] Lari, M. O. and Sahin, A. Z. (2018) "Effect of Retrofitting a Silver/water Nanofluid-Based Photovoltaic/thermal (PV/T) System with a Pcm-Thermal Battery for Residential Applications," Renewable Energy, 122, pp. 98–107. doi: 10.1016/j.renene.2018.01.034.

 [17] Chandrasekar M, Senthilkumar T. Experimental demonstration of enhanced solar energy utilization in flat PV (photovoltaic) modules cooled by heat spreaders in conjunction with cotton wick structures. Energy: part 2. 2015;90:1401-1410. doi:10.1016/j.energy.2015.06.074.

[18] Kandilli, C. (2019) "Energy, Exergy, and Economical Analyses of a Photovoltaic Thermal System Integrated with the Natural Zeolites for Heat Management," *International Journal of Energy Research*, 43(9), pp. 4670–4685. doi: 10.1002/er.4605.

[19] Riverola, A., Mellor, A., Alonso Alvarez, D., Ferre Llin, L., Guarracino, I., Markides, C. N., Paul, D. J., Chemisana, D. and Ekins-Daukes, N. (2018) "Mid-Infrared Emissivity of Crystalline Silicon Solar Cells," Solar Energy Materials and Solar Cells, 174, pp. 607–615. doi: 10.1016/j.solmat.2017.10.002.

[20] 2009 ASHRAE Handbook: Fundamentals - IP Edition. Atlanta: American Society of Heating, Refrigerating and Air-Conditioning Engineers. 2009. ISBN 978-1-933742-56-4.

[21] Huang, M. J., Eames, P. C. and Norton, B. (2004) "Thermal Regulation of Building-Integrated Photovoltaics Using Phase Change Materials," International Journal of Heat and Mass Transfer, 47(12), pp. 2715–2733. doi: 10.1016/j.ijheatmasstransfer.2003.11.015.

[22] Khanjari, Y., Pourfayaz, F. and Kasaeian, A. B. (2016) "Numerical Investigation on Using of Nanofluid in a Water-Cooled Photovoltaic Thermal System," Energy Conversion and Management, 122, pp. 263–278. doi: 10.1016/j.enconman.2016.05.083.

[23] Evans, D. L. (1981) "Simplified Method for Predicting Photovoltaic Array Output," Solar Energy, 27(6), pp. 555–560. doi: 10.1016/0038-092X(81)90051-7.

[24] Holman JP. Experimental methods for engineers. New York: McGraw-Hill;2012.